Prox1-Heterozygosis Sensitizes the Pancreas to Oncogenic Kras-Induced Neoplastic Transformation[1,2]

Yiannis Drosos[*], Geoffrey Neale[†], Jianming Ye[*], Leena Paul[*], Emin Kuliyev[*], Anirban Maitra[‡], Anna L Means[§], M Kay Washington[¶], Jerold Rehg[#], David B Finkelstein[**] and Beatriz Sosa-Pineda[*,††]

[*]Department of Genetics, St. Jude Children's Research Hospital, Memphis, TN; [†]Department of Hartwell Center for Bioinformatics and Biotechnology, St. Jude Children's Research Hospital, Memphis, TN; [‡]The University of Texas MD Anderson Cancer Center, Houston, TX; [§]Department of Cell and Developmental Biology, Vanderbilt University Medical Center, Nashville, TN; [¶]Department of Pathology, Microbiology, and Immunology, Vanderbilt University Medical Center, Nashville, TN; [#]Department of Pathology, St. Jude Children's Research Hospital, Memphis, TN; [**]Department of Computational Biology, St. Jude Children's Research Hospital, Memphis, TN; [††]Department of Medicine, Northwestern University Feinberg School of Medicine, Chicago, IL

Abstract

The current paradigm of pancreatic neoplastic transformation proposes an initial step whereby acinar cells convert into acinar-to-ductal metaplasias, followed by progression of these lesions into neoplasias under sustained oncogenic activity and inflammation. Understanding the molecular mechanisms driving these processes is crucial to the early diagnostic and prevention of pancreatic cancer. Emerging evidence indicates that transcription factors that control exocrine pancreatic development could have either, protective or facilitating roles in the formation of preneoplasias and neoplasias in the pancreas. We previously identified that the homeodomain transcription factor Prox1 is a novel regulator of mouse exocrine pancreas development. Here we investigated whether Prox1 function participates in early neoplastic transformation using in vivo, in vitro and in silico approaches. We found that Prox1 expression is transiently re-activated in acinar cells undergoing dedifferentiation and acinar-to-ductal metaplastic conversion. In contrast, Prox1 expression is largely absent in neoplasias and tumors in the pancreas of mice and humans. We also uncovered that Prox1-heterozygosis markedly increases the formation of acinar-to-ductal-metaplasias and early neoplasias, and enhances features associated with inflammation, in mouse pancreatic tissues expressing oncogenic Kras. Furthermore, we discovered that Prox1-heterozygosis increases tissue damage and delays recovery from inflammation in pancreata of mice injected with caerulein. These results are the first demonstration that Prox1 activity protects pancreatic cells from acute tissue damage and early neoplastic transformation. Additional data in our study indicate that this novel role of Prox1 involves suppression of pathways associated with inflammatory responses and cell invasiveness.

Neoplasia (2016) 18, 172–184

Introduction

Invasive pancreatic ductal adenocarcinoma (PDAC) is among the least curable and most lethal solid malignancies, with patients having a survival rate of less than 4% [1]. PDAC arises from distinct morphologic precursor lesions, of which pancreatic intraepithelial neoplasias (PanINs) are best characterized. PanINs are microscopic papillary or flat, noninvasive ductal intraepithelial neoplasms that, depending on the extent of cytologic atypia, are classified as PanIN-1 (low-grade dysplasia), PanIN-2 (moderate dysplasia), and PanIN-3 (high-grade dysplasia) lesions [2]. PDAC can also originate from other less well-characterized premalignant lesions, including intra-ductal papillary mucinous neoplasms (IPMN) and mucinous cystic neoplasms (MCN) [3].

Recent lineage-tracing studies established that pancreatic acinar cells could give rise to PanINs when exposed to oncogenic Kras activity and inflammation [4]. Acinar cells, the most abundant cell type in the pancreas, are involved in the production of numerous zymogens necessary for nutrient digestion. Adult acinar cells are relatively plastic, and under certain pathologic conditions they dedifferentiate into a progenitor/duct-like lesion called acinar-to-ductal metaplasia (ADM) [4–6]. ADMs are prevalent in individuals with pancreatitis or pancreatic cancer, and it has been proposed that under sustained oncogene stimulation or chronic inflammation these lesions give rise to PanINs [4]. The formation of ADMs involves re-expression of transcription factors (TFs) and components of signaling pathways that normally function in pancreatic progenitors [7–11]. The role of these factors in ADMs is not fully established, but they probably contribute to erase an acinar-differentiation program and to confer plasticity to these structures [7,9,11,12].

Our previous studies identified expression of the homeodomain TF Prox1 in multipotent progenitors, islet cells, and ductal cells in the pancreas of mouse embryos and in most epithelial cells in the pancreas of adult mice, except in acinar cells [13,14]. We also reported that pancreas-specific ablation of Prox1 causes premature acinar cell differentiation [13] and defective ductal morphogenesis at embryonic stages, and promotes acinar cell apoptosis and mild chronic inflammation at postnatal stages [14]. The expression of Prox1 in multipotent progenitors and ductal cells of the pancreas overlaps with that of the One Cut Domain TF Hnf6 [15,16]. Moreover, Prox1 and Hnf6 activities are similarly required for exocrine pancreas develop-ment and some results indicate that in these tissues Hnf6 could function upstream of Prox1 [16]. Interestingly, 2 recent studies showed that Hnf6 expression is upregulated in ADMs of mice and humans [8,10]. These results indicate that Prox1 could be induced together with Hnf6 in ADMs. Moreover, Prox1 activity could play a protective role in neoplastic transformation in the pancreas because a study by Takahashi et al [17] showed that Prox1 ectopic expression suppresses the growth of pancreatic cancer cells.

Here we analyzed the expression of Prox1 in ADMs, neoplasias, and tumors in the pancreas of mice and humans using immuno-staining methods. We also investigated whether Prox1 activity participates in ADM formation using acinar cultures. In addition, we examined the effects of reduced Prox1 activity in oncogene-induced pancreatic transformation using mouse models. Finally, we used comparative gene expression analyses to investigate how Prox1 activity reduces the malignant potential of transformed pancreatic cells. Our study underscored a novel protective role of Prox1 against tissue damage and oncogenic transformation in the mammalian pancreas.

Materials and Methods

Mouse Procedures

Generation of $Prox1^{loxP/+}$ [18], $Ptf1a^{+/cre}$ [19], $Kras^{G12D}$ [20] and *Pdx1-Cre* [21] mice has been described previously. Mice were maintained in a mixed C57/NMRI genetic background. Mice were treated according to the criteria outlined in the Guide for the Care and Use of Laboratory Animals of the National Institutes of Health. All animal experiments were reviewed and approved by the St Jude Animal Care and Use Committee.

Human Tissues

Seven tissue microarrays (TMAs) (total 126 cases) were obtained from the Johns Hopkins Hospital and were stained for PROX1. Additional paraffin sections of human tissues were obtained from the Vanderbilt University Medical Center.

Cell Lines

Capan1, HepG2, MiaPaCa-2, Panc-1 and βTC were obtained from the ATCC and cultured at 37°C, 5% CO_2, and 20% O_2 according to the ATCC guidelines.

Cell Viability Analysis

Capan1 cells maintained in the logarithmic phase of growth were trypsinized, counted, and plated at 500 cells/well in 96-well plates in a total volume of 100 μl of complete medium. Viability was assessed starting on the same day and for 7 more days using the Cell Titer Aqueous Viability assay (Promega) following the manufacturer's instructions.

Acinar Cell Cultures

Primary acinar cells were isolated and cultured as described previously [22]. For RNA isolation, collagen disks were treated with 0.2 mg/mL collagenase P for 10 min, centrifuged at 2000 rpm, and washed twice with HBSS. The cell pellet was resuspended in 350 μL RLT buffer, and total RNA was extracted by using the Qiagen RNeasy Mini Kit. Collagen from BD Biosciences was used to culture acini from *KC* and *KCH* mice, and collagen from Life Sciences was used to culture acini from $Ptf1a^{+/cre}$ mice.

To measure proliferation in ADMs, collagen disks were fixed in 4% PFA for 5 h at 4°C, and embedded in OCT. Thick sections (12 μm) were stained for Ki67 and E-cadherin, and counterstained with DAPI. Ki67+/DAPI+/Ecad+ cells were quantified using ImageJ suite and the cell counter plugin, counting at least 10 microscope fields per genotype.

Immunohistochemical Analysis

Tissue processing and immunostaining were done as described previously [23]. All primary and secondary antibodies used in this study are listed in Supplemental Table 1. Images were obtained with a Zeiss Axioskop 2 microscope, or with a confocal/Multiphoton laser-scanning Zeiss LSM 510 META microscope. Immunohisto-chemically stained slides were further scanned with an Aperio slide scanner (Leica). To measure CD45+ and F4/80+ cells, the algorithm "IHC nuclear staining" was applied on the scanned slides and in the area covering the whole pancreas, excluding the lymph nodes. αSMA+ foci were measured using ImageJ on low magnification images exported from Aperio.

Western Blot Analysis

Whole pancreata from 3-month-old *KC* and *KCH* pancreata were processed as described in [14]. Antibodies used for WB are described

in Supplemental Table 1. Densitometric analysis of digitalized WB images was performed using imageJ software.

Morphometric Analysis and Lesion Scoring

PanIN scoring was performed as previously described [24], with modifications. For each genotype and time point, at least 3 mice of identical genotype were used and pancreas was completely sectioned. For each pancreas, 5 to 7 representative sets consisting of 12 slides each were obtained (each set was separated by 200 µm). After H&E staining of a single section of each set and photomicrography of the whole area (10 to 20 pictures per section), the total area of the section was determined by using the image J software (NIH, http://imagej.nih.gov/ij/). PanINs were counted in each representative section and scored according to their histological characteristics [2]. To measure the number and size of acinar-derived cystic structures (ADMs), the cultures were photographed daily by using the EVOS FL Auto Cell Imaging microscope, and Z-stacks from each culture were obtained. Image J was used to count the total area of each field photographed, the number of ADMs, and the area of each ADM in selected representative images.

RNA Extraction and Quantitative RT-PCR

RNA isolation and cDNA synthesis was performed as previously described [23]. The mRNA levels of each transcript were normalized against the expression of 18sRNA, using the $\Delta\Delta$ct method. $Ptf1a^{+/cre}$ animals were used as controls. All primers used in the study are listed in Supplemental Table 2.

Retroviral Preparation and Capan1 Transduction

The open reading frame (ORF) of human *PROX1* cDNA was cloned into an MSCV-SV40-Puro^R plasmid, and retroviral particles were prepared by tripartite transfection of 293T cells, followed by harvest of viral particles. 293T cells were transfected with either MSCV-Prox1-Puro^R or empty MSCV-SV40-Puro^R vector, and 2 plasmids carrying the viral packaging proteins, by using the CaCl$_2$ method. The supernatant containing viral particles was harvested 24 hours later, filtered through a 0.45-µm gauze filter, and immediately used for transduction. Capan1 cells were transduced with ampho-tropic retroviruses carrying either an MSCV-SV40-Puro^R or an MSCV-Prox1-Puro^R. Two days post-transduction the cells were incubated with 0.5 mg/mL puromycin and selected for 4 days. RNA was isolated from 3 independent transductions with each construct and puromycin selection, using Trizol and the PureLink RNA Mini kit (Life Technologies).

Soft Agar Clonogenic Assay

Capan1 wild type, puro or Prox1-puro cells were mixed in 0.4% Nobleagar (in RPMI supplemented with 10% fetal bovine serum) and plated at 2,500 cells/well onto 6-well plates containing a solidified bottom layer (0.6% Noble agar in the same growth medium). After 21 days, colonies were stained with 0.05% crystal violet and photographed using EVOS. For each experiment, ten low-powered fields (4×) were counted per well.

Immunofluorescence of Cultured Cells

Capan1 cells grown on 4-well chamber slides (Millipore) were fixed with 4% PFA for 15 min at RT, permeabilized and washed with 0.1 % Triton X-100 in PBS, and incubated with primary antibodies and rhodamine-phalloidin in PBS, 3% BSA, 0.1% Triton X-100 for 1 h at RT. Cells were washed with 0.1% Triton X-100, incubated with secondary antibodies in PBS, 3% BSA, 0.1% Triton X-100 for 30 min at RT. Slides were covered with Prolong anti-fade medium plus DAPI and photographed with a Leica DM 2500 confocal microscope.

Microarray Gene Expression Analysis

Total RNA (100 ng) extracted either from Capan1-transduced cells (3 biological replicates of each condition) or pancreata from postnatal day 7 mice was converted into biotin-labeled cRNA (Affymetrix 3'IVT Express Kit, Affymetrix, Inc.) and hybridized to a Human PrimeView GeneChip or to a mouse HT MG-430 PM GeneChip array (Affymetrix, Inc.), respectively. Probe signals from arrays were normalized and transformed into log$_2$ transcript expression values by using the Robust Multi-array Average algorithm [25] (Partek Genomics Suite v6.6). Functional enrichment analysis of gene lists was performed by using the DAVID bioinformatics databases [26] (http://david.abcc.ncifcrf.gov/). Microarray data have been deposited in Gene Expression Omnibus under the accession number GSE58547. FDR was <0.05 except for the genes upregulated in the Capan1-PROX1 analysis where FDR was <0.1.

Caerulein-Induced Pancreatitis

For chemically induced acute pancreatitis, 6- to 8-week-old mice (body weight 20–25 mg) were injected with caerulein (Sigma) as described previously [5], with the following modifications. Each mouse was injected with 72 µg caerulein per kilogram of body weight (10 mg/mL solution) per injection and in total received 8-hourly injections daily for 2 consecutive days. Mice were fasted overnight before the first injection and were returned to the normal feeding schedule after the last injection (d0). For the control experiment, mice of each genotype were injected with the same volume of saline, following the same feeding and injection scheme. Tissues were dissected 7 days post-injections and processed for histologic analysis. To measure serum amylase, 8-week old mice were injected with a single dose of 72 µg/kg body weight of caerulein. After 3 h, retro-orbital blood was collected and submitted to the St. Jude core Pathology lab.

Treatment With 5Aza-dC and TSA

Pancreatic cancer cell lines Capan1 and MiaPaCa2 were treated with 5Aza-dC (Sigma) and TSA (Sigma) as previously described [27]. Cells were exposed continuously to 5Aza-dC (1 µM) for 4 days or to TSA (1 µM) for 24 h. Mock-treated cells were cultured with the equivalent volume of medium, with the addition of equal volume of 50% acetic acid in single-distilled H$_2$O (diluent for 5Aza-dC) or DMSO (diluent for TSA). Cells were harvested at indicated time points, and RNA was extracted as described above.

Prox1 Meta-Analysis

Publically available microarray data from human pancreatic tumors was downloaded from the Gene expression Omnibus (GEO accessions: GSE39751 and GSE28735). The data was controlled for quality using PCA and clinical meta-data to eliminate outliers in Partek Genomics Suite 6.6 (St. Louis MO USA). The highest expressed Prox1 probeset was extracted, examined and plotted with respect to age, gender and other clinical features in STATA/MP11.2 (College Station TX USA).

Statistical Analyses

All statistical analyses were performed by using Microsoft Office Excel and the two-tailed t-test. For all bar graphs, data are presented as

mean ± SEM. Significance was accepted at a *P* value < 0.05. For microarray analysis, differentially expressed transcripts were identified by using the local pooled error (LPE) t-test [28] and the false discovery rate was estimated as described previously [29].

Study Approval

The Johns Hopkins institutional review board (Department of Health and Human Services waiver 4) exempted the TMA analysis of human samples, as it was delinked from human subject identifiers and generated by using archival material from tissues obtained as standard of care. Additional human tissues were obtained with approval from the Vanderbilt University Medical Center IRB.

Results

Prox1 is Expressed in ADMs but not in PanINs and PDAC of Mice and Humans

We investigated the expression of Prox1 in ADMs using immunostaining methods and pancreata of 2 different mouse models: wild-type mice injected with caerulein, and *LSL-Kras*^{G12D}*;Ptf1a*$^{+/cre}$ mice (hereafter named *KC* mice). In the first model, the cholecystokinin analogue caerulein was used to induce mild edematous pancreatitis and extensive ADM formation [30]. In the second model, an oncogenic version of Kras (Kras^{G12D}) was expressed in the pancreas to induce the formation of preneoplasias (including ADMs), PanINs and PDAC, through a disease process that is very similar to that in humans [20,31]. Similar to our published results [13], we detected Prox1 expression in ductal cells and centroacinar cells but not in acinar cells in pancreata of both, caerulein-injected wild-type mice and *KC* mice (Figure 1*A* and data not shown). Also, we observed moderate-to-low Prox1 expression in tubular structures resembling ADMs in pancreata of wild-type mice injected with caerulein (Figure 1*B*). Likewise, we detected Prox1 expression in ductal lesions that occasionally expressed the acinar marker amylase (Figure 1*C*) in pancreata of *KC* mice. These results demonstrate that Prox1 expression is induced in epithelial lesions resembling ADMs in murine pancreatic tissues exposed to acute inflammation or oncogenic stress.

Immunostaining results also showed that PanIN lesions of *KC* mice that were labeled with the specific marker Claudin-18 [23] lacked Prox1 expression, except in those areas that retained normal cuboidal or flat ductal morphology and were Claudin-18 negative (Figure 1*D*). In contrast, PanINs of *KC* mice strongly expressed Sox9 and Hnf1β (Figure 1*E*), 2 TFs that normally co-localize with Prox1 in multipotent progenitors and ductal cells in the pancreas (Supplemental Figure 1). Moreover, in agreement with published data [8,10], we detected Hnf6 expression in early PanINs but not in the more advanced forms of these lesions (data not shown). Immunostaining results also uncovered lack of Prox1 expression in the epithelium of a less frequent neoplasia (IPMN; Figure 1*F*) or in PDAC specimens (Figure 1*G*) of *KC* mice. In contrast, Sox9 and Hnf1β were broadly expressed in IPMNs (Figure 1*F*) and in most PDAC specimens (Figure 1*G*) of *KC* mice. Therefore, we uncovered that Prox1 expression is upregulated in both regenerative lesions (Figure 1*B*) and epithelial structures resembling ADMs (Figure 1*C*), but is not maintained in neoplasias or tumors (Figure 1, *E–G*), in mouse pancreatic tissues expressing Kras^{G12D}.

We also analyzed the expression of PROX1 in neoplasias and tumors of humans using immunostaining methods. Similar to mice,

PROX1 proteins were absent in human PanIN lesions but showed normal distribution in the adjacent islets (Figure 1*H*). Immunostaining of tissue microarrays containing approximately 120 individual human pancreatic tumors showed absence of PROX1 expression in more than 90% of the examined specimens (Figure 1*I* and data not shown). In contrast, the normal-looking ducts, immune cells, and islets surrounding those tumors were positive for PROX1 (Figure 1*H*). Similar to the previous immunostaining results, screening of the human PDAC cell lines Capan1, Panc1, and MiaPaCa2 by quantitative RT-PCR (qRT-PCR) showed very low or no expression of *PROX1* transcripts (Figure 1*J* and data not shown). On the other hand, treatment of Capan1 and MiaPaCa2 cells with the demethylating agent 5-aza-2' deoxycytidine or the histone deacetylase inhibitor trichostatin (Figure 1*K*) increased *PROX1* transcript levels considerably. These results indicate that epigenetic mechanisms contribute to silence *PROX1* expression in pancreatic tumor cells.

Prox1 Heterozygosis Enhances ADM Formation Induced by Oncogenic Kras

Published studies showed that ADM formation requires the activities of Sox9 and Hnf6 [7,8]. Since Prox1 could be part of the same regulatory network involving Sox9 and Hnf6 activities in the pancreas, we investigated whether Prox1 activity plays a role in ADM formation by using a published ex-vivo culture system [22] involving acinar dedifferentiation, cyst formation, loss of acinar markers (e.g., amylase), and induction of cytokeratin-19 (CK-19) and other ductal markers [32]. We focused this and the subsequent analyses on testing the effects of *Prox1*-haploinsufficiency and not complete lack of *Prox1* activity, because full *Prox1* ablation in murine pancreatic progenitors causes extensive loss of acinar tissue and mild chronic inflammation [14]. In contrast, mice carrying *Prox1* heterozygosis in the pancreas (*Ptf1a*$^{+/cre}$*;Prox1*$^{loxP/+}$ mice, hereafter designated *Prox1*$^{Δ/+}$) have intact acinar tissue and do not show any obvious pancreas abnormalities (Supplemental Figure 2).

We harvested the acini from wild-type mice, cultured these tissues for 5 days in three-dimensional collagen gels in the presence of the ADM inducer Transforming Growth Factor alpha (TGFα), and analyzed the resulting cysts by immunostaining. At day 0 of culture, all acinar cells strongly expressed amylase but were devoid of CK-19 expression (Supplemental Figure 3*A*). Also at day 0, most acinar cells were negative for Sox9 or Prox1 expression although a few cells displayed very low levels of these proteins (Supplemental Figure 3*A*). After 5 days of culture the resulting cysts lost amylase expression and became immunopositive for CK19, Sox9 and Prox1 (Supplemental Figure 3*B*). These results show that Prox1 expression is activated in ADMs formed in vitro. We also cultured the acini from *Ptf1a*$^{+/cre}$ mice and *Prox1*$^{Δ/+}$ mice for 5 days in the presence of TGFα and found that the size and number of cysts formed in both genotypes were similar (Supplemental Figure 3*C*). Thus, we conclude that *Prox1* heterozygosis does not affect the ex-vivo formation of ADMs.

Since we found that Prox1 is expressed in ADMs of *KC* pancreata (Figure 1*C*), we investigated whether *Prox1* haploinsufficiency affects ADM formation in the context of oncogenic Kras using acini dissected from *KC* mice and *KCH* mice. *KCH* mice (or *LSL-Kras*^{G12D}*; Ptf1a*$^{+/cre}$*;Prox1*$^{loxP/+}$ mice) carry both Kras^{G12D} expression and ablation of 1 *Prox1* allele in the pancreas. As seen for acini from wild-type mice (Supplemental Figure 3), acini from both *KC* and *KCH* mice that were exposed for 3 days to TGFα produced cysts
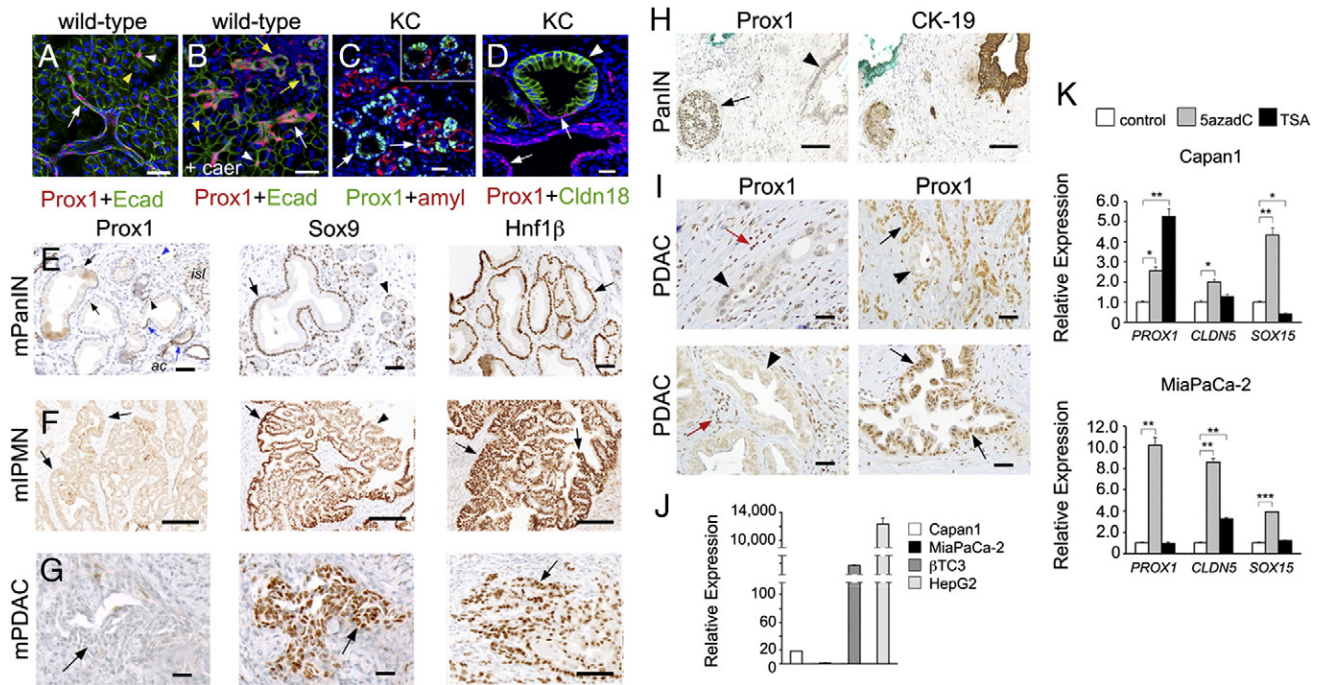
Figure 1. Prox1 is expressed in metaplasias, and is largely undetected in neoplasias and tumors, in murine and human pancreata.A: Prox1 expression is detected in ductal (arrow) and centroacinar cells (arrowhead), but not in acinar cells (yellow arrowhead), in pancreata of wild-type mice.B: Prox1 is expressed in tubular structures (yellow arrows), ducts (white arrow) and centroacinar cells (white arrowhead), in the pancreas of wild-type mice injected with caerulein (yellow arrowhead indicates an acinus).C: ADMs express Prox1 in the pancreas of *KC* mice (arrow and inset).D: Immunostaining for Prox1 and the PanIN-specific tight junction protein Claudin-18 shows near or total absence of Prox1 in PanIN epithelia (arrowhead) of a *KC* pancreatic specimen. Ducts and PanIN areas retaining flat normal-appearing morphology express Prox1 (arrows).E: PanIN-1 areas displaying abundant cytoplasm lack nuclear Prox1 expression (arrows, left) but express Sox9 (arrows, middle) and Hnf1β (arrows, right) in *KC* pancreata. Left panel: Blue arrowheads show Prox1$^+$ cells in PanIN areas displaying normal duct morphology; blue arrowhead indicates a lymphatic vessel. Middle panel: arrowhead indicates a Sox9$^+$ acinus. *isl*, islet; *ac*, acinus.F: Mouse IPMNs display moderate to high expression of Sox9 (arrow, middle) and Hnf1β (arrow, right) and lack Prox1 expression (arrows, left). Arrowhead shows an area of very low Sox9 expression.G: Primary PDAC specimens of *KC* mice express Sox9 (arrow, middle) and Hnf1β (arrow, right) but not Prox1 (arrow, left).H: Adjacent human pancreatic sections demonstrate PROX1 expression in islet cells (arrow) but not in the CK19-positive PanIN epithelium (arrowhead).I: Human PDAC specimens in a tissue microarray show PROX1 expression in normal ducts (black arrows) and immune cells (red arrows). In contrast, except for a few specimens (bottom, right), the glandular epithelium (arrowheads) in most tumors is negative for PROX1.J: Quantitative RT-PCR analysis comparing the relative abundance of *PROX1* transcripts in pancreatic cancer cell lines (Capan1 and MiaPaCa2), insulinoma-derived βTC cells, and the hepatocellular carcinoma cell line HepG2.K: Quantitative RT-PCR results show up-regulation of PROX1 in Capan1 and MIAPaCa-2 cells treated with 5-aza-dC. Trichostatin A (TSA) treatment also increases *PROX1* expression in Capan1 cells. Expression of *CLDN5* and *SOX15*, 2 genes that are hypermethylated in pancreatic cancer cell lines [50], is also induced in Capan1 and MiaPaca-2 cells post-5-aza-dC treatment.Error bars represent ± SEM values (n=3). *P<0.05, **P<0.01 and *** P<0.001. Scale bars: 25 μm (A-D), 50 μm (E-I).

that expressed Prox1, CK19 and Sox9 but were amylase negative (Figure 2*A* and data not shown). Remarkably, we found that the cysts from *KCH* mice were larger (Figure 2, *B* and *C*), expressed substantially more *Cldn18* (Figure 2*D*), were more abundant (Figure 2*E*), and had higher proliferation rates (Figure 2*F*), than the cysts from *KC* mice. These results demonstrate that *Prox1* heterozygosis markedly increases the in vitro formation of ADMs in the context of oncogenic Kras.

Prox1 Heterozygosis Accelerates the Formation of Early Neoplasias, but not Tumor Incidence, in KC Mice

The previous ADM in vitro results suggested that *Prox1* heterozygosis could affect the entire neoplastic process induced by Kras^{G12D}. To investigate this possibility, we dissected the pancreata of *KC* and *KCH* mice at various time points and processed these tissues for histologic and immunostaining analyses. We first analyzed specimens dissected at 1 month because at this age most *KC* mice are

expected to develop numerous preneoplasias and a few early neoplasias (i.e., PanIN-1A) in the pancreas [20]. We found that the areas of desmoplasia encompassing duct-like epithelial structures surrounded by αSMA-positive mesenchymal cells (Figure 3*A*) were more abundant in *KCH* pancreata than in *KC* pancreata (Figure 3*B*) at 1 month of age. On the other hand, the immune infiltrates containing macrophages (F480$^+$ cells) and total leukocytes (CD45$^+$ cells) (Figure 3*A*) were no different between both genotypes at that age (Figure 3*B*). We also analyzed the pancreata of a 2-month old mouse cohort and found that most *KC* pancreatic specimens exhibited an enlarged but still scattered desmoplastic stroma enclosing some low-grade PanINs (Figure 3*C*). In contrast, the areas of desmoplasia were noticeably larger and both the interstitial edema and fibrosis were more prominent in *KCH* pancreata compared to *KC* pancreata (Figure 3*C*) at this age. Also, quantitative results revealed that PanIN-1A, PanIN-1B, and PanIN-2 lesions were significantly more abundant (Figure 3*D*) in *KCH* pancreata than in *KC* pancreata at 2
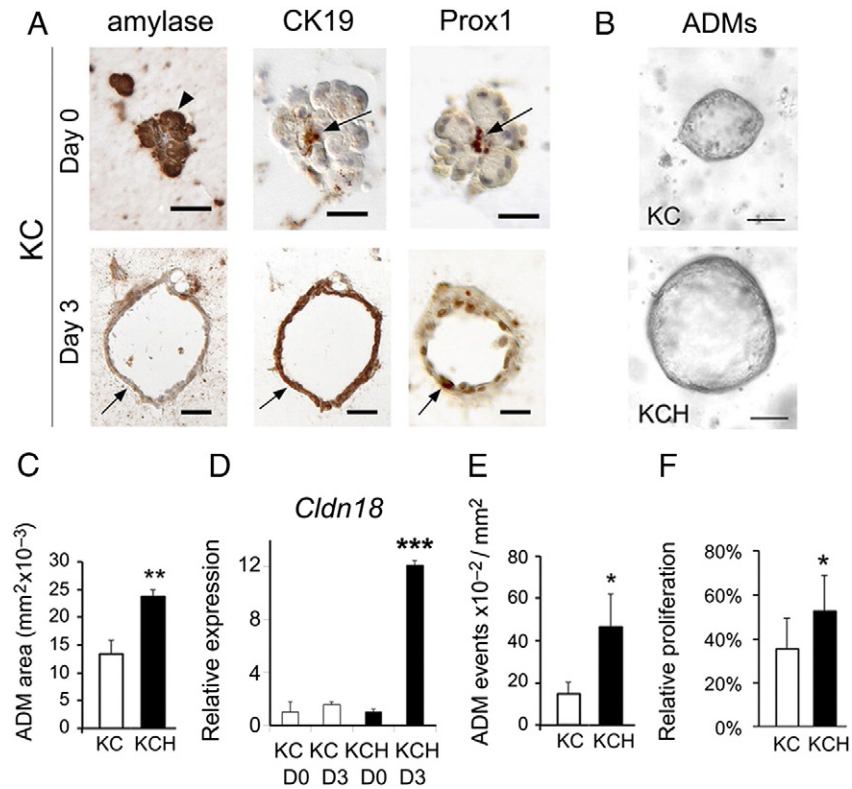
Figure 2. *Prox1* heterozygosis affects the formation of ADMs in the context of oncogenic Kras activity.A: Day 0, Acinar cells (arrowheads) from *KC* pancreata express amylase, but no CK19 or Prox1, at day 0 of culture (arrows indicate CK19$^+$/Prox1$^+$ centroacinar cells). Day 3, *KC* acini cultured for 3 days with TGFα form cysts (arrows) that are negative for amylase and positive for CK19 and Prox1.B, C: *Prox1* heterozygosis increases the size of Kras^{G12D}-expressing acinar-derived cysts after 3 days of culture with TGFα.E: Quantitative PCR results show higher expression of *Cldn18* transcripts in *KCH* versus *KC* acinar cultures treated for 3 days with TGFα. Error bars represent $\pm$ SEM values (n=3-4 individual specimens per time point).E, F: *Prox1* heterozygosis increases the number and proliferation rate of Kras-^{G12D}-expressing acinar-derived cysts cultured for 3 days with TGFα.*P<0.05, **P<0.01 and *** P<0.001.

months. Furthermore, these results were reproduced in a separate cohort of *KC* and *KCH* mice that were generated using a different Cre parental strain (*Pdx1-Cre*, Figure 3F) [21]. Altogether, these data demonstrate that *Prox1*-heterozygosis accelerates early neoplastic transformation induced by Kras^{G12D} in mouse pancreata.

We also compared the incidence of pancreatic tumors in 2 cohorts of *KC* and *KCH* mice (n= 12 in each group) that were euthanized at 13–15 months of age (except for 1 *KCH* mouse that was found moribund at 7 months). We uncovered that 3 mice in the *KCH* group developed an IPMN lesion whereas only 1 mouse in the *KC* group displayed a similar neoplasia (Figure 4A, Supplemental Table 3). These results corroborate that *Prox1* heterozygosis accelerates the formation of Kras^{G12D}-induced neoplasias. On the other hand, we found that each of 4 *KC* mice and 4 *KCH* mice developed pancreatic tumors surrounded by high-grade PanIN-3 lesions (Supplemental Table 3 and data not shown). Histologic and immunostaining analyses of the tumors identified 2 nonmetastatic PDACs in the *KC* group and 3 PDACs (2 nonmetastatic and 1 metastatic) in the *KCH* group (Figure 4B). In addition, a longitudinal study performed in a separate cohort of *KC* and *KCH* mice (n= 16 in each group) showed no differences in survival in both genotypes (Figure 4C). Thus, *Prox1* haploinsufficiency does not affect pancreatic tumor incidence in mice. We hypothesize that once specific tumor suppressors are inactivated or certain oncogenic mutations are acquired, Prox1 downregulation becomes irrelevant for the transformation process.

Prox1 Heterozygosis Sensitizes the Pancreas to the Effects of Caerulein Administration

Histology results revealed that the interstitial edema and fibrosis were more prominent in pancreatic tissues of *KCH* mice compared to *KC* mice (Figure 3C). Also, Western blot results showed that phospho-Smad3 (a TGF-β effector) and phospho-p65 (the active form of the p65/p50 NF-κB complex) proteins were more abundant in pancreata of *KCH* mice than of *KC* mice (Figure 5, *A* and *B*). In contrast, there were no differences in total p65, phospho-STAT3, and phospho-Akt proteins between pancreata of either genotype (Figure 5, *A* and *B*). These results indicate that *Prox1* heterozygosis increases features associated with inflammation in pancreatic tissues expressing oncogenic Kras. Therefore, we hypothesized that *Prox1* heterozygosis might influence the response of the pancreas to other stressors that trigger injury and inflammation. We explored this possibility by comparing the effects of caerulein administration between *Ptf1a*$^{+/cre}$ mice and *Prox1*$^{Δ/+}$ mice.

Exposure to caerulein increases amylase levels in the blood, causes acinar cell death, and leads to a transient inflammatory pathology that is reminiscent of acute-pancreatitis [30]. We injected *Ptf1a*$^{+/cre}$ mice and *Prox1*$^{Δ/+}$ mice with a single dose of saline or caerulein and measured serum amylase levels 3 hours post-administration. Compared with saline, caerulein increased serum amylase levels by 1.7- fold in *Ptf1a*$^{+/cre}$ mice (P = 0.095) and by 2.8-fold in *Prox1*$^{Δ/+}$ mice (P=0.038; Figure 5C). Therefore, the acinar damage inflicted by
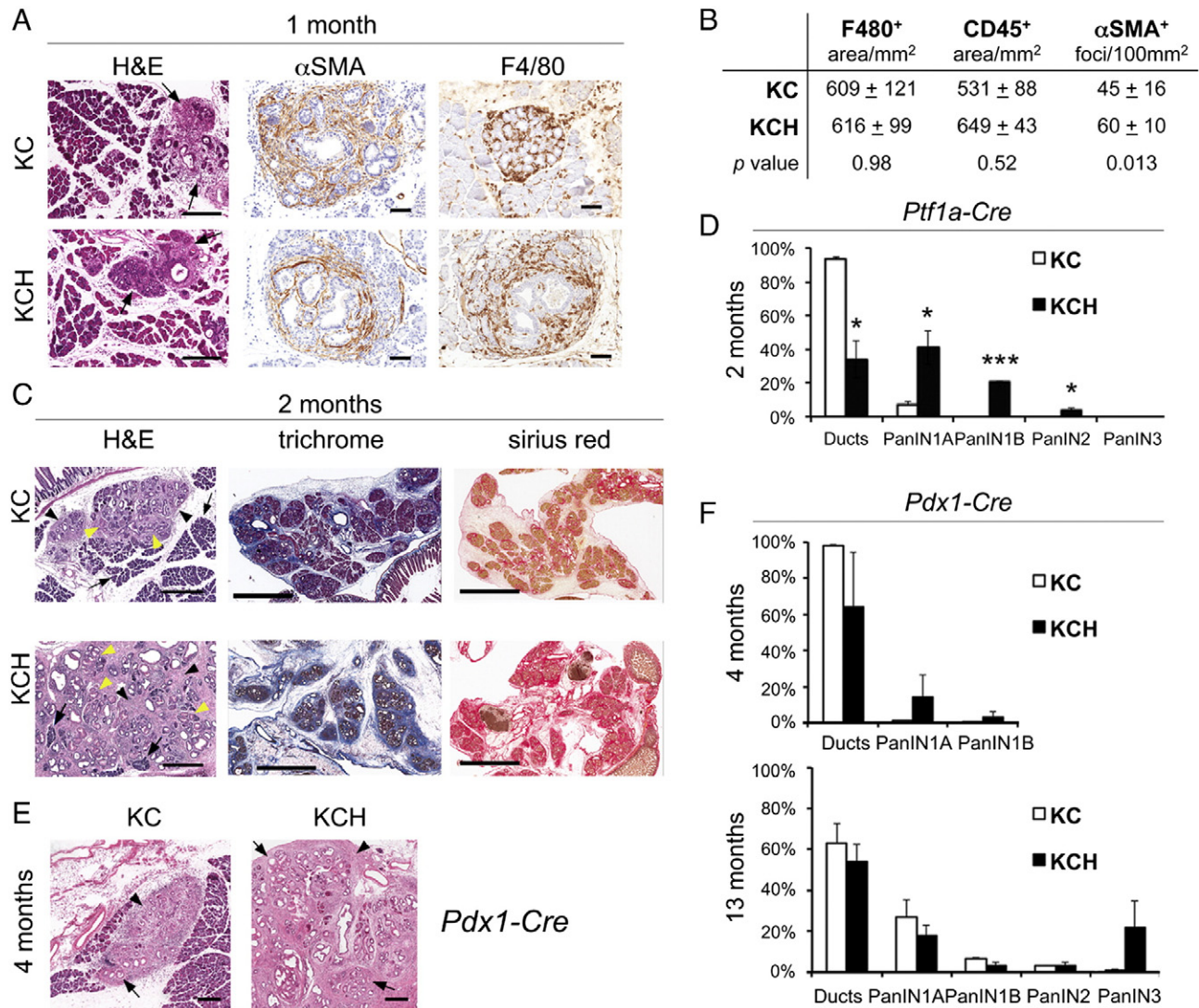
Figure 3. *Prox1* heterozygosis accelerates early transformation downstream of Kras[G12D].A: Small areas of desmoplasia (arrows) are noticeable in *KC* and *KCH* pancreata at 1 month (H&E). These foci include atypical flat epithelial lesions surrounded by abundant stellate cells (αSMA$^+$) and infiltrating macrophages (F4/80$^+$). Scale bars: 50 μm.B: Quantification of macrophage-positive (F4/80) and total leukocyte-positive (CD45) areas shows no difference between *KC* and *KCH* pancreata at 1 month. In contrast, αSMA$^+$ foci are more abundant in the *KCH* specimens.C: (H&E staining) Two-months old *KC* pancreata have few foci of desmoplasia (arrowheads) harboring ADMs, and a few PanIN lesions (yellow arrows) surrounded by large portions of normal-looking tissue (arrow). In comparison, 2-month old *KCH* pancreata have more numerous PanINs (yellow arrows), more abundant desmoplasia (arrowheads), and less intact acinar tissue (arrows). Features associated with inflammation (i.e., interstitial edema and fibrosis [trichrome and Sirius red staining]), are more prominent in *KCH* pancreata than in *KC* pancreata at 2 months. Scale bars: 400 μm (H&E), 3 mm (trichrome and Sirius red).D: Quantitative comparison of the proportion of normal ducts and PanINs between pancreata of 2-month old *KC* and *KCH* mice (*Ptf1a-Cre*).E: (H&E staining) The pancreata of 4-month old *KCH* mice that were offspring of *Pdx1-Cre* (B6C57) breeders displays larger areas of desmoplasia (arrowheads) and more numerous PanIN lesions (arrows) in comparison to pancreata of *KC* littermates. Scale bars: 200 μm.F: Quantitative comparison of the proportion of normal ducts and PanINs between pancreata of 4-month old *KC* and *KCH* mice (mice were produced using *Pdx1-Cre* [B6C57] breeders).Error bars represent $\pm$ SEM values from (n=3) individual pancreatic specimens per genotype. *$P<0.05$, *** $P<0.001$.

caerulein was more profound in *Prox1*$^{\Delta/+}$ mice than in *Ptf1a*$^{+/cre}$ mice. We also compared the recovery of *Prox1*$^{\Delta/+}$ and *Ptf1a*$^{+/cre}$ pancreatic tissues from caerulein administration using histologic and immunostaining methods. Consistent with the serum amylase results, various features indicative of inflammation (e.g., edema, and total leukocyte and macrophage infiltration) were more acute in the pancreas of *Prox1*$^{\Delta/+}$ mice 7 days after caerulein administration (Figure 5, *D* and *E*) than in pancreata of similarly treated *Ptf1a*$^{+/cre}$ mice. These results demonstrate that *Prox1* heterozygosis increases

tissue injury and delays recovery from inflammation in pancreatic tissues exposed to caerulein.

Prox1 Activity Reduces Anchorage-Independent Growth and Gene Signatures Associated With Cell Transformation, Invasiveness and Inflammation, in Pancreatic Cancer Cells

Our results from both mice injected with caerulein and *KC* mice indicated that Prox1 activity participates in processes that protect pancreatic cells from tissue injury and oncogenic transformation. To
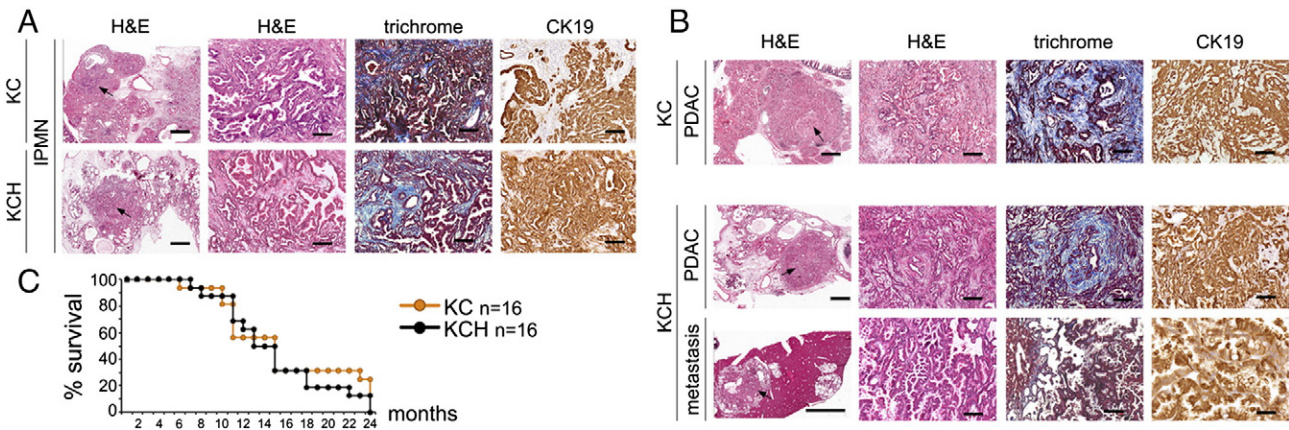
Figure 4. *Prox1* heterozygosis does not affect pancreatic tumor formation downstream of oncogenic Kras or survival outcome in mice.A: H&E staining reveals a high-grade IPMN (arrows) in each of *KC* and *KCH* pancreata. The IPMNs express CK19 and are surrounded by a collagen-positive desmoplasia (trichrome staining).B: *KC*, H&E staining shows the characteristic glandular architecture of a non-invasive PDAC (the CK19 expression confirms its ductal identity). *KCH*, An invasive PDAC displays glandular morphology (H&E) and expresses CK19. The liver metastasis also expresses CK19 and show histologic features of both adenocarcinoma and IPMN. Trichrome staining reveals abundant collagen deposition around the primary tumors.C: Kaplan-Meier curves show similar survival outcome for *KC* and *KCH* mice (n=16 per genotype).Scale bars: 100 μm (A, B: second, third and fourth columns), 1mm (A, first column and B, first column [except bottom image that is 3mm]).

begin dissecting this novel role of Prox1, we induced its ectopic expression in the human pancreatic tumor cell line Capan1 using retroviral vectors, and compared the morphology, growth and gene expression profiles between PROX1-Capan1 cells and Capan1 cells infected with control viruses. Morphologic analyses using bright microscopy revealed membranous extensions resembling filopodia in most control-Capan1 cells (Figure 6A). In contrast, PROX1-Capan1 cells had very small filopodia or completely lacked these structures (Figure 6A). Also, staining for F-actin showed prominent distribution of filamentous actin at the leading edge in control-Capan1 cells and more compact distribution in peripheral PROX1-Capan1 cells (Figure 6B). Furthermore, staining with E-cadherin antibodies showed that this protein was restricted to cells located in the center in control-Capan1 cultures, whereas most cells in the PROX1-Capan1 cultures strongly expressed E-cadherin (Figure 6C). These results demonstrate that PROX1 activity reduces morphologic traits associated with cell adhesion and migration in pancreatic tumor cells.

Takahashi et al [17] showed that PROX1 ectopic expression decreases growth in MiaPaCa2 cells. Similarly, using an ATP-based viability assay we uncovered that ectopic PROX1 expression reduced the expansion of Capan1 cells (Figure 6D). Furthermore, colony agar formation assay results showed that Capan1 cells that expressed PROX1 had significantly lower anchorage-independent growth in comparison to control Capan1 cells (Figure 6E). These results further prove that Prox1 activity reduces the malignant potential of transformed pancreatic cells. To gain mechanistic insight into this effect of Prox1 function, the gene expression profiles of PROX1-Capan1 cells and control-Capan1 cells were compared using Affymetrix arrays. This analysis uncovered >2-fold significant upregulation of 216 genes, and >2-fold significant downregulation of 480 genes, in PROX1-Capan1 cells compared to control-Capan1 cells (Figure 5F). Results of gene ontology analysis showed significant enrichment of epithelial development and regulation of cell proliferation pathways within the genes that were upregulated in PROX1-Capan1 cells (Supplemental Table 4). QRT-PCR results confirmed the upregulation of some of these genes in Capan1 cells virally transduced with

PROX1 (Supplemental Figure 4), but the reciprocal effect was not observed in pancreatic tissues from *KCH* mice (data not shown). Therefore, we conclude that Prox1 increased the former genes in cooperation with factors that are specific to Capan1 cells.

Both gene ontology and qRT-PCR results revealed that functions involving wound healing, chemotaxis, cell adhesion, cell motility, and inflammation (Figures 6F and 7A, and Supplemental Table 4) were significantly downregulated in PROX1-Capan1 cells. QRT-PCR analysis of various candidates selected from the PROX1-Capan1–downregulated data sets showed that proinflammatory transcripts (*Reg3b, Saa1, Nfkbiz, Il-6, Cxcl2, Cxcl3, Ccl5, Il1rl1*), transcripts that promote tumor invasiveness (*Mmp9, Mmp1, Plat, Plau, Plaur*), and transcripts associated with pancreatic neoplastic transformation (*S100a9, Cd44, Cldn2, Cldn18*), were substantially increased in *KC* pancreata compared to *Ptf1a⁺/cre* (control) pancreata (Figure 7B). More remarkably, results from similar analyses revealed that numerous transcripts involved with functions that were downregulated in PROX1-Capan1 cells, had significantly higher expression in *KCH* pancreata compared to *KC* pancreata (Figure 7B) at 1 month of age. Likewise, we found that the ADMs from *KCH* mice expressed considerably higher levels of the proinflammatory transcripts *Il-6, Saa1* and *Cxcl3*; the tumor invasiveness-related transcripts *Mmp9, Plau, Plaur* and *Plat*; and the PanIN-specific transcript *Cldn18* (Figures 2D and 7C), in comparison to ADMs from *KC* mice. These results establish that Prox1 activity suppresses pathways that confer invasiveness and pathways involved with inflammation in transformed pancreatic cells.

Discussion

Acinar plasticity manifests in response to injury or stress to help repair the damaged tissue and to facilitate regeneration. In rodents (and probably also in humans) afflicted with pancreatitis the acinar cells transiently de-differentiate and undergo ADM conversion, a process that reverts once the damage and inflammation subside. However, under pathologic conditions associated with sustained inflammation or oncogenic stress this course is derailed and the progression of
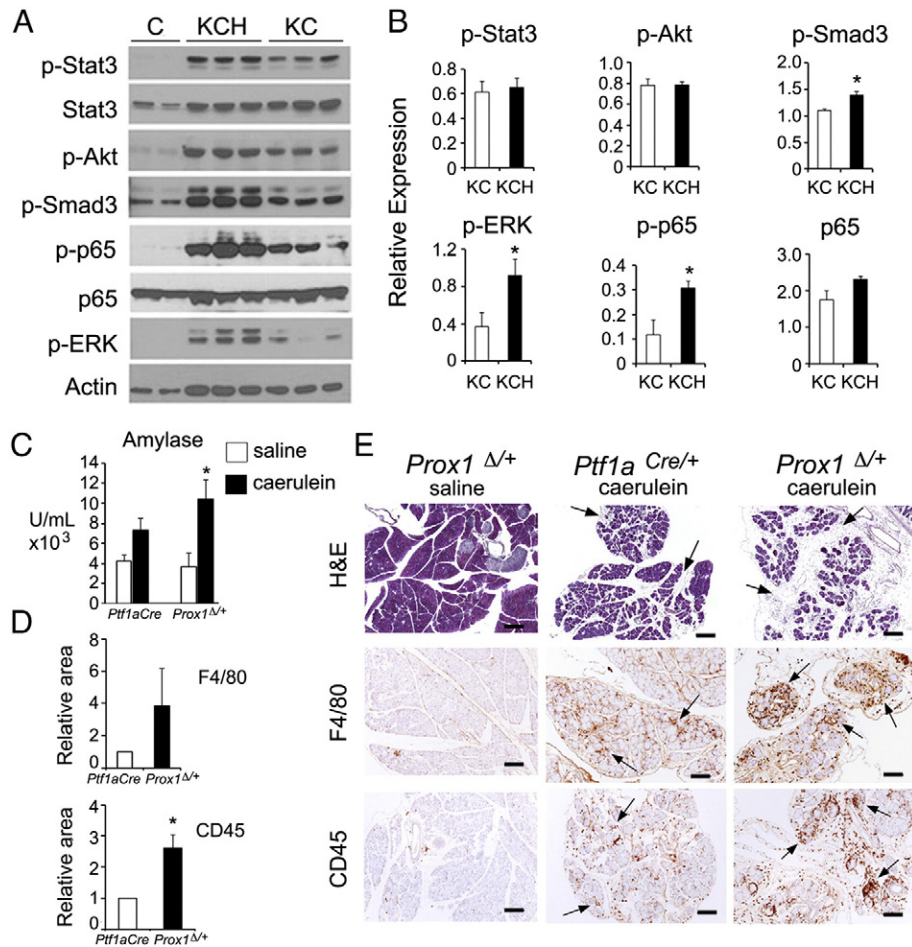
Figure 5. *Prox1* heterozygosis accentuates tissue damage and inflammation triggered by caerulein or Kras[G12D].A, B: Western blot (A) and densitometry analysis (B) showing expression of markers associated with inflammation and transformation downstream of Kras[G12D] activity. β actin served as loading control. Phospho-p65 and phospho-Stat3 values were calculated relative to their total levels whereas the rest of the proteins were calculated relative to β actin. The pancreatic tissues were harvested at 3 months of age.C: Serum amylase increases more in *Prox1* [/+] mice than in *Ptf1a* [+/cre] mice 3 hours after a single injection of caerulein (72 μg/kg body weight).D: Infiltrates of both macrophage (F4/80-immunopositive) and total leukocytes (CD45-immunopositive) are more abundant in *Prox1* [/+] pancreata than in *Ptf1a* [+/cre] pancreata, 7 days post-caerulein administration.E: *Prox1* [/+] pancreata have more prominent interstitial edema (H&E staining) and more immune infiltrates (i.e., F4/80^{+} cells and CD45^{+} cells, arrows) than *Ptf1a* [+/cre] pancreata 7 days post-caerulein injection. *Prox1* [/+] pancreata injected with saline have normal morphology and do not display features of inflammation (scale bars: 200 μm).Error bars represent $\pm$ SEM values from ((n=3 [B], n=4 [C, saline], n=6 [C, caerulein], and n=3 (D)] specimens per genotype. *$P < 0.05$.

ADMs into precancerous neoplasias is favored [33]. The formation of ADMs is accompanied by reactivation of a "progenitor signature" involving TFs and signaling pathways that normally are expressed in embryonic pancreatic precursors [5,6,34]. Our study uncovered that Prox1 is a novel component of the previous "progenitor signature", and revealed that its function limits the development of ADMs and the formation of pancreatic neoplasias in the setting of oncogenic Kras.

Although currently we do not know the functional outcome of Prox1 induction in wild-type ADMs, we hypothesize that this step could help to disassemble the program of acinar differentiation because we previously showed that Prox1 activity opposes acinar development in pancreatic progenitors [13]. Moreover, Prox1 induction could help conferring "progenitor/ductal" characteristics to ADMs as we previously described that Prox1 activity is necessary for ductal development [14]. This potential role of Prox1 would be similar to that proposed for Hnf6, a TF though to function in the

same pathway as Prox1 in pancreatic ductal cells [14–16] and whose induction in ADMs was shown to decrease acinar gene expression [8]. Further studies should clarify the functional significance of Prox1 expression in non-transformed ADMs.

While Prox1 induction probably assists the initial steps of ADMs conversion, we found that its activity also posses a barrier for the progression of ADMs into neoplasias in the context of oncogenic Kras. This latter function may be due both to indirect effects on the microenvironment (discussed below) and to cell autonomous effects on epithelial character. Not only did loss of one *Prox1* allele result in greater numbers of early neoplastic lesions in vivo, it also led to elevated expression of *Cldn18* in isolated acini that were induced to undergo ADM in vitro. Claudin-18 is one of few markers that distinguish ADMs from early neoplastic lesions. Thus, reduction of Prox1 enables transition from benign to neoplastic disease in the models shown here.
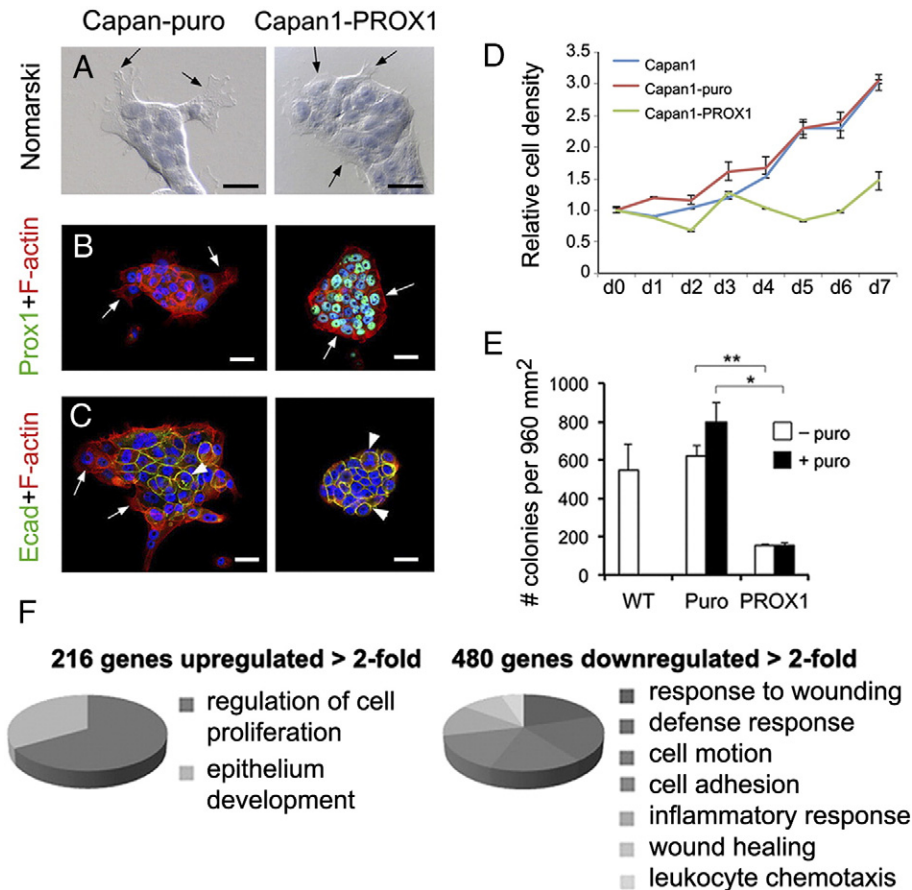
Figure 6. PROX1 ectopic expression decreases the transforming potential of Capan1 cells.A: Nomarski images of cells counterstained with hematoxylin show conspicuous cell protrusions (arrows) in Capan1-puro cells but not in Capan1-PROX1 cells. Scale bars: 40 μm.B, C: Co-staining for F-actin/Prox1 (B) and F-actin/E-cadherin (C) depicts focal and cell-cell adhesions in Capan1-PROX1 cells and Capan1-puro cells (arrows indicate cell protrusions and arrowheads adherent junctions). Scale bars: 40 μm.D: Capan1-PROX1 cells display reduced expansion in comparison to Capan1 cells and Capan1-puro cells. Data were generated from 3 individual cultures.E: Capan1-PROX1 cells produced significantly fewer colonies in soft agar assays compared to Capan1-puro cells. Data were generated from 2 independent experiments, each in triplicate (error bars = mean $\pm$ SD). *$P<0.05$, **$P<0.01$.F: Results of Gene Ontology analysis showed that 216 genes were upregulated $>$ 2-fold and 480 genes were downregulated $>$ 2-fold, in Capan1-PROX1 cells vs. Capan1-puro cells. Functions associated with epithelium development and cell proliferation were enriched in the upregulated genes, and functions associated with inflammation, wound healing, cellular motion and cell adhesion were enriched in the downregulated genes.

We hypothesize that sustained Prox1 activity could induce pathways leading to cell cycle arrest or senescence in ADMs that express Kras^{G12D}, since we found that *KCH* acini produced larger and more proliferative cysts than *KC* acini. A similar role for Prox1 was proposed in the developing lens where its loss of function caused abnormal cell proliferation and downregulation of the cell-cycle inhibitors p57 and p27 [35]. Moreover, a recent study showed that in lens epithelial cells expressing H-ras^{G12V}, Prox1 expression was upregulated together with p57 and p27 [36]. This potential negative effect of Prox1 activity for Kras^{G12D}-induced transformation would explain why this TF is downregulated in early neoplasias. Therefore, one could envision that in acini undergoing metaplastic conversion Prox1 is initially induced to help establishing a "progenitor/ductal state", but as the Kras-induced oncogenic program process advances loss of Prox1 expression enables progression from ADM to PanIN. Our future efforts should attempt to identify the mechanism(s) responsible for silencing Prox1 expression in PanINs. In this regards, it is intriguing that Prox1 transient expression in ADMs is identical to

that of Hnf6 because other studies concluded that Hnf6 might act upstream of Prox1 in pancreatic tissues [8,15,16].

Another important effect of *Prox1* heterozygosis is that this condition increased the focal areas of desmoplasia, the number of preneoplasias, and features of inflammation, in the pancreata of young *KC* mice. These alterations could result from enhanced expression of proinflammatory proteins (e.g., *Il-6*, encoding a potent activator of pancreatic stellate cells [37], metalloproteases, plasminogen activators, and other proteins known to participate in neoplastic transformation and tissue repair [38–41] in ADMs that carry reduced Prox1 dosage. In addition, Prox1 heterozygosis could have influenced the transformation of acinar cells in a non-cell autonomous manner by increasing the production of proinflammatory and other tumor-promoting factors in ductal cells. The notion that Prox1 regulates similar processes in transformed ADMs and in pancreatic ductal cells is intriguing because Prox1 is continuously expressed in the pancreatic ducts and these structures are highly refractory to Kras^{G12D}–induced transformation [7]. Future studies using
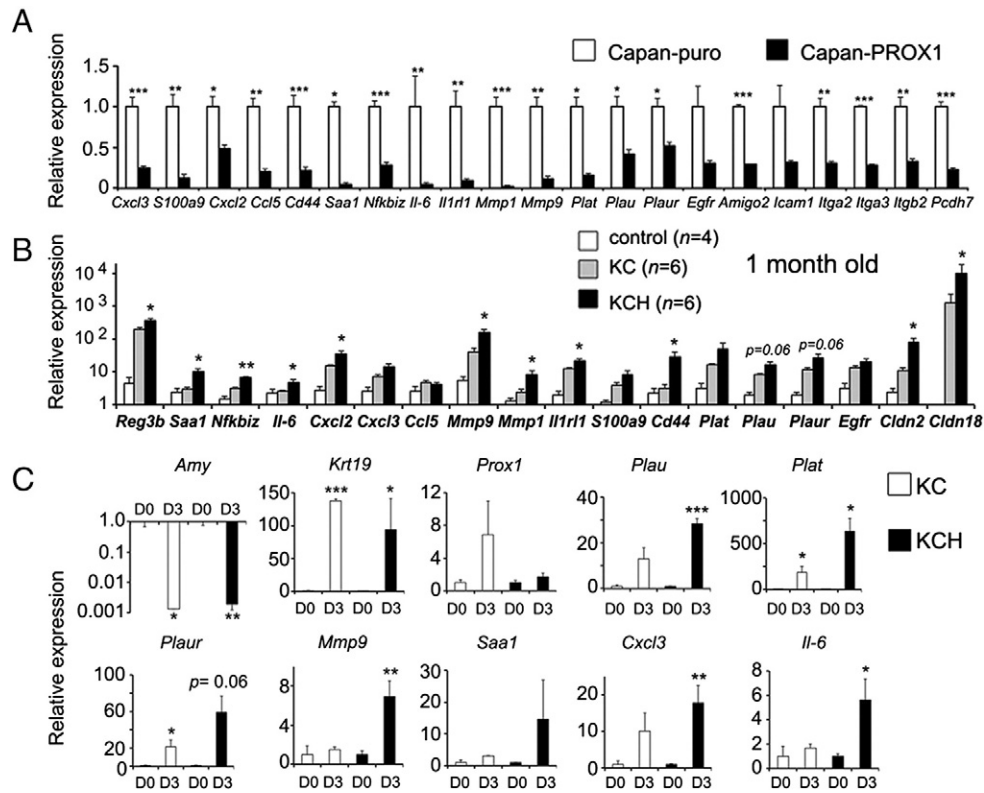
Figure 7. *Prox1*-heterozygosis increases the expression of transcripts encoding proteins associated with inflammation and transformation in Kras^G12D-pancreatic tissues.A: Quantitative PCR confirms expression changes in Capan1-PROX1 cells of downregulated genes selected from the pathway enrichment analyses.B: Quantitative PCR shows higher expression of several transcripts identified in the Capan1-PROX1 microarray, in pancreata of 1-month old *KCH* mice in comparison to those tissues of *Ptf1a* ^+/cre^ (control) or *KC* mice (asterisks compare *KC* versus *KCH* results).C: Quantitative PCR results show variable expression of transcripts selected from the Capan1-PROX1 expression analysis, in acinar cultures prepared from *KC* and *KCH* pancreata. Acini from *KC* and *KCH* pancreata show similar changes in the transcription of Amylase (down) and Ck19 (up) after 3 days in culture. *Prox1* transcripts show marked upregulation in *KC* acinar cultures but not in *KCH* cultures between days 0 and 3. *Plau*, *Plat*, *Plaur*, *Mmp9*, *Saa1*, *Cxcl3* and *Il-6* transcripts show higher upregulation in *KCH* tissues compared to *KC* tissues during the culture period.Error bars represent $\pm$ SEM values from: (n=3) independent viral transduction experiments in Capan1-PROX1 cells and Capan1-puro cells (A), (n=4-6) individual pancreatic tissues (B), and (n=3-4) individual cultures per time point (C).*$P<0.05$, **$P<0.01$ and ***$P<0.001$.

conditional deletion approaches should clarify how Prox1 activity affects the susceptibility of acinar and ductal cells to oncogenic transformation.

Inflammation plays a key role in pancreatic repair by eliminating injured cells and promoting epithelial renewal [42,43]. However, inflammation also contributes to various important aspects of pancreatic tumorigenesis such as: facilitating ADM and PanIN formation [44,45], inducing epithelial-to-mesenchymal transition at the PanIN stage [46], promoting desmoplasia [43,47], and amplifying Kras activity to pathologic levels [48]. The strong reliance of Kras^G12D-driven transformation on inflammatory stimuli explains why pathologic conditions such as chronic pancreatitis increase the risk for pancreatic cancer [49]. We found that *Prox1* heterozygosis enhanced several features associated with inflammation in a mouse model of pancreatic cancer induced by oncogenic Kras (e.g., desmoplasia, fibrosis, and expression of phospho-Smad3 and phospho-p65 proteins) and in a mouse model of caerulein-induced pancreatitis (e.g., persistence of immune infiltrates). Furthermore, Prox1 could directly repress inflammatory pathways in pancreatic cells because we identified Prox1-binding sites in regulatory regions of various NF-κB target genes (data not shown). Our future efforts will

try to identify the mechanisms downstream of Prox1 activity responsible for protection from excessive injury and attenuation of inflammatory responses in the pancreas. This information should have therapeutic relevance because it could identify processes or factors that could be targeted at the early stages of the neoplastic process. Furthermore, our study predicts that the effects of pancreatitis or oncogenic transformation are more severe in individuals carrying reduced dosage of PROX1 in the pancreas.

Another major conclusion of our study is that Prox1 activity does not seem to play a role in pancreatic tumor formation but rather in the initiation of the process. In fact, similar to the report of the Takahashi lab [17], we determined that Prox1 expression is negligible or completely absent in neoplasias and tumors in the pancreas of mice and humans. Moreover, although in a few human PDAC specimens we detected moderate-to-low PROX1 protein expression, our results of in silico analyses of published databases did not reveal significant correlation between PROX1 expression levels and the differentiation status of pancreatic tumors or patient survival (data not shown). It remains to be determined whether PROX1 is functionally inactive in tumors that express this protein or if certain PDAC mutations offset the activity of this transcription factor (e.g., like those described by

Takahashi et al in *PROX1* RNA, [17]), especially since we found that PROX1 ectopic expression lessens the transforming potential of pancreatic cancer cells. Identifying the specific effectors downstream of Prox1 activity that reduce invasiveness and traits associated with transformation in pancreatic tumor cells could open new therapeutic opportunities and help restraining the metastatic potential of this devastating form of cancer.

In summary, we discovered that Prox1 heterozygosis sensitizes the pancreas to excessive damage and inflammation caused by injury or oncogenic stress. Our findings predict that dissecting the mechanism(s) behind this novel role of Prox1 should help the diagnosis and treatment of some pathologic conditions that predispose to pancreatic cancer in humans.

Authors' Contributions

BS-P and YD conceived, designed, and directed the study and wrote the manuscript. YD performed most of the experiments with the assistance of LP, JY and EK. GN and DBF assisted with the analysis of microarray data. AM evaluated the mouse tumor results and provided and evaluated the human TMA. ALM and MKW provided human tissue samples and assisted with histologic evaluation. JR assisted with evaluation of mouse tumors.

Acknowledgements

Appendix A. Supplementary Data

Supplementary data to this article can be found online at http://dx.doi.org/10.1016/j.neo.2016.02.002.

References

[1] Siegel R, Ma J, Zou Z, and Jemal A (2014). Cancer statistics, 2014. *CA Cancer J Clin* **64**(1), 9–29.

[2] Hruban RH, Adsay NV, Albores-Saavedra J, Compton C, Garrett ES, Goodman SN, Kern SE, Klimstra DS, Kloppel G, and Longnecker DS, et al (2001). Pancreatic intraepithelial neoplasia: a new nomenclature and classification system for pancreatic duct lesions. *Am J Surg Pathol* **25**(5), 579–586.

[3] Hidalgo M (2012). New insights into pancreatic cancer biology. *Ann Oncol* **23**(Suppl. 10), x135–x138.

[4] Puri S, Folias Alexandra E, and Hebrok M (2015). Plasticity and Dedifferentiation within the Pancreas: Development, Homeostasis, and Disease. *Cell Stem Cell* **16**(1), 18–31.

[5] Jensen JN, Cameron E, Garay MV, Starkey TW, Gianani R, and Jensen J (2005). Recapitulation of elements of embryonic development in adult mouse pancreatic regeneration. *Gastroenterology* **128**(3), 728–741.

[6] Pinho AV, Rooman I, Reichert M, De Medts N, Bouwens L, Rustgi AK, and Real FX (2011). Adult pancreatic acinar cells dedifferentiate to an embryonic progenitor phenotype with concomitant activation of a senescence programme that is present in chronic pancreatitis. *Gut* **60**(7), 958–966.

[7] Kopp JL, von Figura G, Mayes E, Liu FF, Dubois CL, Morris JPt, Pan FC, Akiyama H, Wright CV, and Jensen K, et al (2012). Identification of Sox9-dependent acinar-to-ductal reprogramming as the principal mechanism for initiation of pancreatic ductal adenocarcinoma. *Cancer Cell* **22**(6), 737–750.

[8] Prevot PP, Simion A, Grimont A, Colletti M, Khalaileh A, Van den Steen G, Sempoux C, Xu X, Roelants V, and Hald J, et al (2012). Role of the ductal transcription factors HNF6 and Sox9 in pancreatic acinar-to-ductal metaplasia. *Gut* **61**(12), 1723–1732.

[9] Flandez M, Cendrowski J, Canamero M, Salas A, del Pozo N, Schoonjans K, and Real FX (2014). Nr5a2 heterozygosity sensitises to, and cooperates with, inflammation in KRas(G12V)-driven pancreatic tumourigenesis. *Gut* **63**(4), 647–655.

[10] Pekala KR, Ma X, Kropp PA, Petersen CP, Hudgens CW, Chung CH, Shi C, Merchant NB, Maitra A, and Means AL, et al (2014). Loss of HNF6 expression correlates with human pancreatic cancer progression. *Lab Invest* **94**(5), 517–527.

[11] von Figura G, Morris JPt, Wright CV, and Hebrok M (2014). Nr5a2 maintains acinar cell differentiation and constrains oncogenic Kras-mediated pancreatic neoplastic initiation. *Gut* **63**(4), 656–664.

[12] Krah NM, De La OJ, Swift GH, Hoang CQ, Willet SG, Chen Pan F, Cash GM, Bronner MP, Wright CV, and MacDonald RJ, et al (2015). The acinar differentiation determinant PTF1A inhibits initiation of pancreatic ductal adenocarcinoma. *Elife* **4**.

[13] Wang J, Kilic G, Aydin M, Burke Z, Oliver G, and Sosa-Pineda B (2005). Prox1 activity controls pancreas morphogenesis and participates in the production of "secondary transition" pancreatic endocrine cells. *Dev Biol* **286**(1), 182–194.

[14] Westmoreland JJ, Kilic G, Sartain C, Sirma S, Blain J, Rehg J, Harvey N, and Sosa–Pineda B (2012). Pancreas-Specific Deletion of Prox1 Affects Development and Disrupts Homeostasis of the Exocrine Pancreas. *Gastroenterology* **142**(4), 999–1009 [e1006].

[15] Pierreux CE, Poll AV, Kemp CR, Clotman F, Maestro MA, Cordi S, Ferrer J, Leyns L, Rousseau GG, and Lemaigre FP (2006). The Transcription Factor Hepatocyte Nuclear Factor-6 Controls the Development of Pancreatic Ducts in the Mouse. *Gastroenterology* **130**(2), 532–541.

[16] Zhang H, Ables ET, Pope CF, Washington MK, Hipkens S, Means AL, Path G, Seufert J, Costa RH, and Leiter AB, et al (2009). Multiple, temporal-specific roles for HNF6 in pancreatic endocrine and ductal differentiation. *Mech Dev* **126**(11–12), 958–973.

[17] Takahashi M, Yoshimoto T, Shimoda M, Kono T, Koizumi M, Yazumi S, Shimada Y, Doi R, Chiba T, and Kubo H (2006). Loss of function of the candidate tumor suppressor prox1 by RNA mutation in human cancer cells. *Neoplasia* **8**(12), 1003–1010.

[18] Harvey NL, Srinivasan RS, Dillard ME, Johnson NC, Witte MH, Boyd K, Sleeman MW, and Oliver G (2005). Lymphatic vascular defects promoted by Prox1 haploinsufficiency cause adult-onset obesity. *Nat Genet* **37**(10), 1072–1081.

[19] Kawaguchi Y, Cooper B, Gannon M, Ray M, MacDonald RJ, and Wright CV (2002). The role of the transcriptional regulator Ptf1a in converting intestinal to pancreatic progenitors. *Nat Genet* **32**(1), 128–134.

[20] Hingorani SR, Petricoin EF, Maitra A, Rajapakse V, King C, Jacobetz MA, Ross S, Conrads TP, Veenstra TD, and Hitt BA, et al (2003). Preinvasive and invasive ductal pancreatic cancer and its early detection in the mouse. *Cancer Cell* **4**(6), 437–450.

[21] Gu G, Dubauskaite J, and Melton DA (2002). Direct evidence for the pancreatic lineage: NGN3+ cells are islet progenitors and are distinct from duct progenitors. *Development* **129**(10), 2447–2457.

[22] Means AL, Meszoely IM, Suzuki K, Miyamoto Y, Rustgi AK, Coffey Jr RJ, Wright CV, Stoffers DA, and Leach SD (2005). Pancreatic epithelial plasticity mediated by acinar cell transdifferentiation and generation of nestin-positive intermediates. *Development* **132**(16), 3767–3776.

[23] Westmoreland JJ, Drosos Y, Kelly J, Ye J, Means AL, Washington MK, and Sosa-Pineda B (2012). Dynamic distribution of claudin proteins in pancreatic epithelia undergoing morphogenesis or neoplastic transformation. *Dev Dyn* **241**(3), 583–594.

[24] De La OJ, Emerson LL, Goodman JL, Froebe SC, Illum BE, Curtis AB, and Murtaugh LC (2008). Notch and Kras reprogram pancreatic acinar cells to ductal intraepithelial neoplasia. *Proc Natl Acad Sci U S A* **105**(48), 18907–18912.

[25] Irizarry RA, Hobbs B, Collin F, Beazer-Barclay YD, Antonellis KJ, Scherf U, and Speed TP (2003). Exploration, normalization, and summaries of high density oligonucleotide array probe level data. *Biostatistics* **4**(2), 249–264.

[26] Huang da W, Sherman BT, and Lempicki RA (2009). Systematic and integrative analysis of large gene lists using DAVID bioinformatics resources. *Nat Protoc* **4**(1), 44–57.

[27] Sato N, Fukushima N, Maitra A, Matsubayashi H, Yeo CJ, Cameron JL, Hruban RH, and Goggins M (2003). Discovery of novel targets for aberrant methylation in pancreatic carcinoma using high-throughput microarrays. *Cancer Res* **63**(13), 3735–3742.

[28] Jain N, Thatte J, Braciale T, Ley K, O'Connell M, and Lee JK (2003). Local-pooled-error test for identifying differentially expressed genes with a small number of replicated microarrays. *Bioinformatics* **19**(15), 1945–1951.

[29] Benjamini Y, Drai D, Elmer G, Kafkafi N, and Golani I (2001). Controlling the false discovery rate in behavior genetics research. *Behav Brain Res* **125**(1-2), 279–284.

[30] Lerch MM and Gorelick FS (2013). Models of Acute and Chronic Pancreatitis. *Gastroenterology* **144**(6), 1180–1193.

[31] Albury TM, Pandey V, Gitto SB, Dominguez L, Spinel LP, Talarchek J, Klein-Szanto AJ, Testa JR, and Altomare DA (2015). Constitutively Active Akt1 Cooperates with KRasG12D to Accelerate In Vivo Pancreatic Tumor Onset and Progression. *Neoplasia* **17**(2), 175–182.

[32] Pan FC and Wright C (2011). Pancreas organogenesis: From bud to plexus to gland. *Dev Dyn* **240**(3), 530–565.

[33] Stanger BZ and Hebrok M (2013). Control of Cell Identity in Pancreas Development and Regeneration. *Gastroenterology* **144**(6), 1170–1179.

[34] Esni F, Ghosh B, Biankin AV, Lin JW, Albert MA, Yu X, MacDonald RJ, Civin CI, Real FX, and Pack MA, et al (2004). Notch inhibits Ptf1 function and acinar cell differentiation in developing mouse and zebrafish pancreas. *Development* **131**(17), 4213–4224.

[35] Wigle JT, Chowdhury K, Gruss P, and Oliver G (1999). Prox1 function is crucial for mouse lens-fibre elongation. *Nat Genet* **21**(3), 318–322.

[36] Burgess D, Zhang Y, Siefker E, Vaca R, Kuracha MR, Reneker L, Overbeek PA, and Govindarajan V (2010). Activated Ras alters lens and corneal development through induction of distinct downstream targets. *BMC Dev Biol* **10**, 10–13.

[37] Mews P, Phillips P, Fahmy R, Korsten M, Pirola R, Wilson J, and Apte M (2002). Pancreatic stellate cells respond to inflammatory cytokines: potential role in chronic pancreatitis. *Gut* **50**(4), 535–541.

[38] Wang W, Abbruzzese JL, Evans DB, and Chiao PJ (1999). Overexpression of urokinase-type plasminogen activator in pancreatic adenocarcinoma is regulated by constitutively activated RelA. *Oncogene* **18**(32), 4554–4563.

[39] Gironella M, Calvo C, Fernandez A, Closa D, Iovanna JL, Rosello-Catafau J, and Folch-Puy E (2013). Reg3beta deficiency impairs pancreatic tumor growth by skewing macrophage polarization. *Cancer Res* **73**(18), 5682–5694.

[40] Xue A, Chang JW, Chung L, Samra J, Hugh T, Gill A, Butturini G, Baxter RC, and Smith RC (2012). Serum apolipoprotein C-II is prognostic for survival after pancreatic resection for adenocarcinoma. *Br J Cancer* **107**(11), 1883–1891.

[41] Jiang W, Zhang Y, Kane KT, Collins MA, Simeone DM, di Magliano MP, and Nguyen KT (2015). CD44 Regulates Pancreatic Cancer Invasion through MT1-MMP. *Mol Cancer Res* **13**(1), 9–15.

[42] Folias AE, Penaranda C, Su AL, Bluestone JA, and Hebrok M (2014). Aberrant Innate Immune Activation following Tissue Injury Impairs Pancreatic Regeneration. *PLoS ONE* **9**(7), e102125.

[43] Gukovsky I, Li N, Todoric J, Gukovskaya A, and Karin M (2013). Inflammation, autophagy, and obesity: common features in the pathogenesis of pancreatitis and pancreatic cancer. *Gastroenterology* **144**(6), 1199–1209 [e1194].

[44] Liou GY, Doppler H, Necela B, Krishna M, Crawford HC, Raimondo M, and Storz P (2013). Macrophage-secreted cytokines drive pancreatic acinar-to-ductal metaplasia through NF-kappaB and MMPs. *J Cell Biol* **202**(3), 563–577.

[45] Liou G-Y, Doppler H, Necela B, Edenfield B, Zhang L, Dawson DW, and Storz P (2015). Mutant Kras-induced expression of ICAM-1 in pancreatic acinar cells causes attraction of macrophages to expedite the formation of precancerous lesions. *Cancer Discov* **5**(1), 52–63.

[46] Rhim AD, Mirek ET, Aiello NM, Maitra A, Bailey JM, McAllister F, Reichert M, Beatty GL, Rustgi AK, and Vonderheide RH, et al (2012). EMT and dissemination precede pancreatic tumor formation. *Cell* **148**(1-2), 349–361.

[47] Botta GP, Reichert M, Reginato MJ, Heeg S, Rustgi AK, and Lelkes PI (2013). ERK2-regulated TIMP1 Induces Hyperproliferation of K-Ras(G12D)-Transformed Pancreatic Ductal Cells. *Neoplasia* **15**(4), 359–372.

[48] Daniluk J, Liu Y, Deng D, Chu J, Huang H, Gaiser S, Cruz-Monserrate Z, Wang H, Ji B, and Logsdon CD (2012). An NF-kappaB pathway-mediated positive feedback loop amplifies Ras activity to pathological levels in mice. *J Clin Invest* **122**(4), 1519–1528.

[49] Pinho AV, Chantrill L, and Rooman I (2014). Chronic pancreatitis: A path to pancreatic cancer. *Cancer Lett* **345**(2), 203–209.

[50] Vincent A, Omura N, Hong SM, Jaffe A, Eshleman J, and Goggins M (2011). Genome-wide analysis of promoter methylation associated with gene expression profile in pancreatic adenocarcinoma. *Clin Cancer Res* **17**(13), 4341–4354.